Formation of Grignard Species from the Reaction of Methyl Halides with Laser-Ablated Magnesium Atoms. A Matrix Infrared Study of CH_3MgF, CH_3MgCl, CH_3MgBr, and CH_3MgI

William D. Bare and Lester Andrews*

Contribution from the Department of Chemistry, University of Virginia, Charlottesville, Virginia 22901

Received March 10, 1998

Abstract: Magnesium atoms generated by laser ablation were reacted with methyl halides diluted (0.5% to 0.1%) in argon. Reaction products were trapped in a cryogenic argon matrix and analyzed by infrared spectroscopy. The primary reaction product, isolated Grignard molecule CH_3MgX, and the secondary reaction products MgX, MgX_2, MgH, MgH_2, CH_4, C_2H_6, CH_2X, CH_3MgCH_3, $XMgCH_2$, $HMgCH_3$, and $HMgCH_2X$ were identified by isotopic (^{13}C, D, and ^{26}Mg) substitution and by correlation with B3LYP and BP86 isotopic frequency calculations. This investigation reports the first experimental evidence for the fluoride Grignard species, CH_3MgF. Infrared absorptions were also observed for associated Grignard species.

Introduction

Alkylmagnesium halides, Grignard reagents, are among the most synthetically useful compounds available to organic chemists. Surprisingly, although it has been nearly one hundred years since Grignard's first report[1] of the synthesis and general utility of these species, many aspects of the mechanism of Grignard formation remain poorly understood. Grignard formation reactions have been widely investigated, and this study continues that work with laser-ablated magnesium atoms.

Grignard compounds are most commonly prepared by reaction of magnesium metal with alkyl halides dissolved in ether or tetrahydrofuran. The formation and structures of side-products in these reactions is clear evidence of the involvement of radical species as intermediates. It is generally accepted that an electron is transferred from the metal surface to the alkyl halide, forming an alkyl halide radical anion, which subsequently dissociates to give an alkyl radical and a halide ion. The halide ion is associated with the electron-deficient metal surface, presumably forming MgX. Ultimately, the alkyl radical combines with MgX radical to give the Grignard complex. In recent years, investigations have focused on the nature of the alkyl radical precursors in Grignard formation reactions and have attempted to determine whether these species remain closely associated with the metal surface[2] or diffuse freely in solution[3] prior to radical addition. Most recently, investigators have studied the nature of the reactive sites on the metal surface, concluding that Grignard formation is strongly influenced by characteristics of the metal surface,[4] and is likely initiated at crystal defects or impurities in the metal.

The importance of the nature of the metal substrate is further supported by UV−vis and IR matrix-isolation studies of thermally evaporated magnesium co-condensed with methyl halides.[5−9] UV−vis experiments by Imizu and Klabunde[5] have shown that magnesium clusters (Mg_n, where $n = 2$, 3, or 4) are more reactive toward alkyl halides than are ground-state magnesium atoms. Ault[6] and Solov'ev et al.[7] have performed IR experiments with thermally evaporated magnesium and methyl chloride, methyl bromide, or methyl iodide, and have identified Grignard species as products. Unfortunately, this technique produced broad IR bands, and comparatively few of the CH_3MgX vibrational modes could be conclusively assigned. Of greater importance, it will be shown here that broad bands assigned previously to Grignard species[6,7] are not the isolated molecule but aggregated species.

Matrix isolation has also been used to investigate the possible formation of dimagnesium Grignard species.[7] Ab initio and density functional theory (DFT) calculations have predicted that reactions of alkyl halides (RX) with magnesium clusters may yield alkyldimagnesium halide species (RMgMgX and RMgXMg), which are expected to be more stable than their monomagnesium analogues.[10−13] Attempts to produce and observe such species, however, have thus far been unsuccessful.[7]

With these results in mind, we have undertaken an investigation of the reaction of the methyl halides, CH_3F, CH_3Cl, CH_3Br, and CH_3I, with energetic magnesium atoms produced by

(1) Grignard, V. (Jones, P. R.; Southwick, E., translation.) *J. Chem. Educ.* **1970**, *47*, 291.
(2) Walborsky, H. M.; Zimmermann, C. *J. Am. Chem. Soc.* **1992**, *114*, 4996. Walborsky, H. M.; Topolski, M. *J. Am. Chem. Soc.* **1992**, *114*, 3455. Walborsky, H. M.; Rachon, J. *J. Am. Chem. Soc.* **1989**, *111*, 1896.
(3) Garst, J. F.; Ungvary, F.; Baxter, J. T. *J. Am. Chem. Soc.* **1997**, *119*, 253. Garst, J. F.; Ungvary, F.; Batlaw, B.; Lawrence, K. E. *J. Am. Chem. Soc.* **1991**, *113*, 5392. Root, K. S.; Hill, C. L.; Lawrence, L. M.; Whitesides, G. M. *J. Am. Chem. Soc.* **1989**, *111*, 5405. Ashby, E. C.; Oswald, J. *J. Org. Chem.* **1988**, *53*, 6068.
(4) Teerlinck, C. E.; Bowyer, W. J. *J. Org. Chem.* **1996**, *61*, 1059. Koon, S. E.; Oyler, C. E.; Hill, J. H. M.; Bowyer, W. J. *J. Org. Chem.* **1993**, *58*, 3225.
(5) Imizu, Y.; Klabunde, K. J. *Inorg. Chem.* **1984**, *23*, 3602.
(6) Ault, B. S. *J. Am. Chem. Soc.* **1980**, *102*, 3480.
(7) Solov'ev, V. N.; Sergeev, G. B.; Nemukhin, A. V.; Burt, S. K.; Topol, I. A. *J. Phys. Chem. A* **1997**, *101*, 8625.
(8) Tanaka, Y.; Davis, S. C.; Klabunde, K. J. *J. Am. Chem. Soc.* **1982**, *104*, 1013.
(9) Klabunde, K. J.; Whetten, A. *J. Am. Chem. Soc.* **1986**, *108*, 6529.
(10) Nemukhin, A. V.; Solov'ev, V. N.; Sergeev, G. B.; Topol, I. A. *Mendeleev Commun.* **1996**, *1*, 5.
(11) Nemukhin, A. V.; Topol, I. A.; Weinhold, F. *Inorg. Chem.* **1995,** *34*, 2980.
(12) Jaisen, P. G.; Dykstra, C. E. *J. Am. Chem. Soc.* **1983**, *105*, 2089.
(13) Jaisen, P. G.; Dykstra, C. E. *J. Am. Chem. Soc.* **1985**, *107*, 1891.

S0002-7863(98)00806-3 CCC: $15.00
Published on Web 07/10/1998

laser ablation.[14] The higher kinetic and electronic energy of the laser-ablated atoms (vis a vis thermal atoms) enables reactions to be investigated with methyl fluoride, which, owing to the comparatively high H_3C-F bond strength, is the least reactive alkyl halide in Grignard formation. Past matrix isolation infrared studies have not included reactions with CH_3F. Herein are reported the analysis of infrared spectra of the reaction products of laser-ablated magnesium atoms with CH_3F, CH_3Cl, CH_3Br, and CH_3I diluted in argon and condensed at 10 K.

Experimental Section

The apparatus used for laser ablation and matrix isolation of products has been described previously.[15] Methyl fluoride (Matheson), methyl chloride (Matheson), methyl bromide (Matheson), and methyl iodide (Aldrich) samples were diluted with argon (Airco) to yield 1/200 or 1/400 (CH_3X:Ar) mixtures. Methyl iodide liquid was purified by 2 freeze−pump−thaw cycles prior to use; other gases were used as received. A magnesium (Fisher) disk, mounted on a rotating rod, was ablated by a focused Nd:YAG laser (1064 nm) with a pulse rate of 10 Hz and with energy of 20−50 mJ/pulse. Gas mixtures were deposited on a 10 ± 1 K CsI window at a rate of 2 mmol/h for 90 min, during ablation of the magnesium target. Reaction products were co-condensed with argon on the cold window, and infrared spectra were recorded with a Nicolet 750 Fourier transform infrared spectrophotometer with 0.5 cm^{-1} resolution. After initial spectra were recorded, the matrixes were subjected to stepwise annealing to 25, 30, and 35 K, with spectra recorded after each cycle. Matrices were also subjected to broad-band photolysis from a medium-pressure Hg arc lamp (Philips 175W, with glass globe removed). Spectra were recorded after photolysis. Experiments were repeated with isotopically enriched samples, including ^{26}Mg (Oak Ridge National Laboratory, >95% ^{26}Mg), CD_3Br (MSD Isotopes), CD_3F (prepared as described previously[16]), and $^{13}CH_3F$ (MSD Isotopes).

Calculations

DFT calculations were performed on reagent molecules and on expected products with the Gaussian94 program[17] operating on an SP2 computer. Calculations were done with use of the BP86 and B3LYP functionals[18−21] with 6-311+G* basis sets.[22,23] Correlation with observed spectra of methyl halide molecules in argon has demonstrated that these functionals with the 6-311+G* basis set provide accurate (generally better than ±4%) frequency calculations for these molecules. Calculated and observed frequencies for CH_3F are shown in Table 1 for comparison. The B3LYP functional produces frequencies in better agreement with the observed values than the BP86 functional. Calculations were performed on methyl iodide and iodine-containing products with D95 basis sets for C and H, 6-311 for Mg, and the LanL2Z basis set and pseudopotentials for iodine. Initial calculations for CH_3MgX molecules allowing maximum geometric freedom converged to C_{3v} symmetry within experimental error. In subsequent calculations, C_{3v} symmetry was imposed by defining C−Mg−X bond angles as 180.0° and appropriate dihedral angles as 120.0°. The B3LYP and BP86 functionals produced slightly different frequencies, as listed in Table 2, but the shifts between the calculated isotopic frequencies were essentially the same.

Table 1. DFT Calculated and Observed Vibrational Frequencies (cm^{-1}) of Methyl Fluoride. (Calculated Intensities (km/mol) Are in Parentheses)

	calcd		obsd	
mode	BP86/ 6-311+G*	B3LYP/ 6-311+G*	gas phase[a]	in solid argon
sym C−F str (a_1)	1004.4 (114)	1034.7 (122)	1048.2	1039.9
Me rock (e)	1155.6 (0.3)	1195.6 (0.8)	1195.5	1182.9
sym Me def (a_1)	1442.0 (2)	1492.0 (2)	1475.3	1462.4[b]
antisym Me def (e)	1456.2 (5)	1506.4 (5)	1471.1	1462.4[b]
sym C−H str (a_1)	2953.6 (38)	3042.6 (35)	2864.5	2968.4
antisym C−H str (e)	3041.8 (40)	3129.1 (38)	2982.2	3017.6

[a] Gas−phase data from ref 35. [b] A broader band at 1462.4 cm^{-1} probably contains both a_1 and e modes. Overtone bands are observed at 2863.3 and 2914.5 cm^{-1} in solid argon.

Nemukhin and co-workers have previously reported calculations on CH_3F, on CH_3MgF, and on CH_3Cl, CH_3MgCl, CH_3Br, and CH_3MgBr, all done at Hartree−Fock level with 6-31G* basis sets.[10,11] Saikai and Jordan have reported similar calculations,[24] and Solov'ev and co-workers have presented Hartree−Fock calculations with MP2 corrections and DFT calculations using B3P86 and B3LYP functionals for CH_3Cl, CH_3MgCl, CH_3Br, and CH_3MgBr, including some calculations with large (6-311++G**) basis sets.[7] DFT calculations on CH_3MgF and CH_3MgI have not previously been reported. DFT calculated geometries and frequencies for methylmagnesium halide molecules, including CH_3MgF and CH_3MgI, are given in Table 2.

Results

Experiments were conducted with laser-ablated magnesium atoms (^nMg or ^{26}Mg) and CH_3F, CD_3F, $^{13}CH_3F$, CH_3Cl, CH_3Br, CD_3Br, and CH_3I. Spectra from these experiments are shown in Figures 1−4, and IR absorptions are listed in Tables 3−6. Bold letters in the text refer to labels in these figures; all bands labeled "**P**" are due to the parent methyl halide molecules, and those labeled "**G**" are due to Grignard molecules.

It is almost universally true that product bands formed in these experiments were observed immediately following deposition and were not significantly affected by photolysis or by first (25, 30 K) annealing. These bands generally decreased 15 to 20% on subsequent 35 K annealing. This describes the behavior of all IR bands observed here, unless stated otherwise.

Mg + CH_3X. Reaction of methyl halide molecules with magnesium produced several IR bands, which exhibited no shift as a function of halogen substitution. These bands were observed in reactions with at least three methyl halides and are listed in Table 3.

Methane and ethane are expected products for these reactions, and bands in these experiments were compared to infrared spectra of samples of dilute methane and ethane in argon. Accordingly, bands at 1305.4 and 3036.5 cm^{-1} are assigned to methane. Weak halogen-independent bands at 818.2, 820.3, 822.2, 1374.6, 1464.3, 1466.1, 1467.9, 2891.4, and 2979.7 cm^{-1} are similarly assigned to ethane.

A sharp, weak band (**A**) was observed at 502.2 cm^{-1} and shifted to 492.1 cm^{-1} with $^{13}CH_3F$. A similar sharp 502.2 cm^{-1} band was observed by Greene et al.[25] in experiments with laser-ablated magnesium and methane.

(14) Kang, H.; Beauchamp, J. L *J. Phys. Chem.* **1985**, *89*, 3364.
(15) Burkholder, T. R.; Andrews, L *J. Chem. Phys.* **1991**, *95*, 8679. Hassenzadeh, P.; Andrews, L. *J. Phys. Chem.* **1992**, *96*, 9177.
(16) Andrews, L.; Dyke, J. M.; Jonathan, N.; Keddar, N.; Morris, A.; Ridha, A. *J. Phys. Chem.* **1984**, *88*, 2364.
(17) Gaussian 94, Revision B.1, Frisch, M. J.; Trucks, G. W.; Schlegel, H. B.; Gill, P. M. W.; Johnson, B. G.; Robb, M. A.; Cheeseman, J. R.; Keith, T.; Petersson, G. A.; Montgomery, J. A.; Raghavachari, K.; Al-Laham, M. A.; Zakrzewski, V. G.; Ortiz, J. V.; Foresman, J. B.; Cioslowski, J.; Stefanov, B. B.; Nanayakkara, A.; Challacombe, M.; Peng, C. Y.; Ayala, P. Y.; Chen, W.; Wong, M. W.; Andres, J. L.; Replogle, E. S.; Gomperts, R.; Martin, R. L.; Fox, D. J.; Binkley, J. S.; Defrees, D. J.; Baker, J.; Stewart, J. P.; Head-Gordon, M.; Gonzalez, C.; Pople, J. A.; Gaussian, Inc.: Pittsburgh, PA, 1995.
(18) Lee, C.; Yang, W.; Parr, R. G. *Phys. Rev. B* **1988**, *37*, 785.
(19) Becke, A. D. *J. Chem. Phys.* **1993**, *98*, 5648.
(20) Becke, A. D. *Phys. Rev. A* **1988**, *38*, 3098.
(21) Perdew, J. P. *Phys. Rev. B* **1986**, *33*, 8822.
(22) McLean, A. D.; Chendler, G. S. *J. Chem. Phys.* **1980**, *72*, 5639.
(23) Krishnan, R.; Binkley, J. S.; Seeger, R.; Pople, J. A. *J. Chem. Phys.* **1980**, *72*, 650.
(24) Sakai, S.; Jordan, K. D. *J. Am. Chem. Soc.* **1982**, *104*, 4019.
(25) Greene, T.; Lanzisera, D.; Andrews, L.; Downs, A. J. *J. Am. Chem. Soc.* **1998**, *120*, 6097.

Table 2. DFT Calculated Frequencies (cm^{-1}), Intensities (km/mol), and Geometries[a] (Å, deg) for Methyl Magnesium Halides with BP86 and B3LYP Functionals and 6-311+G* Basis Sets[b]

	CH_3MgF		CH_3MgCl		CH_3MgBr		CH_3MgI	
	BP86	B3LYP	BP86	B3LYP	BP86	B3LYP	BP86[b]	B3LYP[b]
C−Mg−X bend (e)	130.5 (52)	133.8 (56)	113.2 (31)	118.0 (34)	104.3 (24)	108.0 (27)	91.2 (18)	94.9 (21)
sym C−Mg−X str (a_1)	456.0 (0.7)	467.2 (0.7)	357.5 (17)	366.0 (17)	290.3 (16)	296.1 (17)	232.9 (15)	237.3 (16)
Me rock (e)	597.4 (95)	611.4 (97)	594.4 (79)	610.2 (80)	591.3 (72)	607.2 (73)	649.3 (87)	660.7 (90)
antisym C−Mg−X str (a_1)	733.0 (104)	755.1 (109)	609.7 (92)	623.5 (95)	587.7 (78)	600.7 (80)	582.7 (41)	595.9 (42)
sym Me def (a_1)	1149.4 (0.0)	1195.4 (0.0)	1145.7 (0.2)	1197.6 (0.0)	1148.0 (0.7)	1196.5 (0.3)	1185.5 (0.7)	1230.2 (1.5)
antisym Me def (e)	1430.1 (0.1)	1477.6 (0.1)	1427.2 (0.3)	1476.1 (0.3)	1427.9 (0.4)	1476.4 (0.4)	1439.9 (3.3)	1481.8 (3.9)
sym C−H str (a_1)	2940.6 (25)	3012.5 (28)	2944.9 (27)	3011.7 (31)	2943.1 (29)	3009.9 (34)	2951.7 (32)	3019.7 (37)
antisym. C−H str (e)	3016.6 (14)	3082.6 (16)	3022.7 (13)	3081.6 (16)	3020.0 (13)	3080.1 (16)	3056.5 (19)	3119.0 (22)
r(Mg−X)	1.807	1.793	2.224	2.215	2.371	2.363	2.641	2.631
r(C−Mg)	2.090	2.083	2.089	2.081	2.091	2.082	2.077	2.068
r(C−H)	1.104	1.095	1.103	1.095	1.103	1.095	1.108	1.100
∠(Mg−C−H)	111.8	111.7	111.6	111.7	111.7	111.7	110.9	110.9

[a] Methyl magnesium halide molecules were confined to C_{3v} symmetry and C−Mg−X bond angle defined as 180.0°. [b] Basis sets used for methyl magnesium iodide were the following: 6-311 for Mg, D95 for C and H, and LanL2Z for I. LanL2Z effective core potentials were also used for iodine.

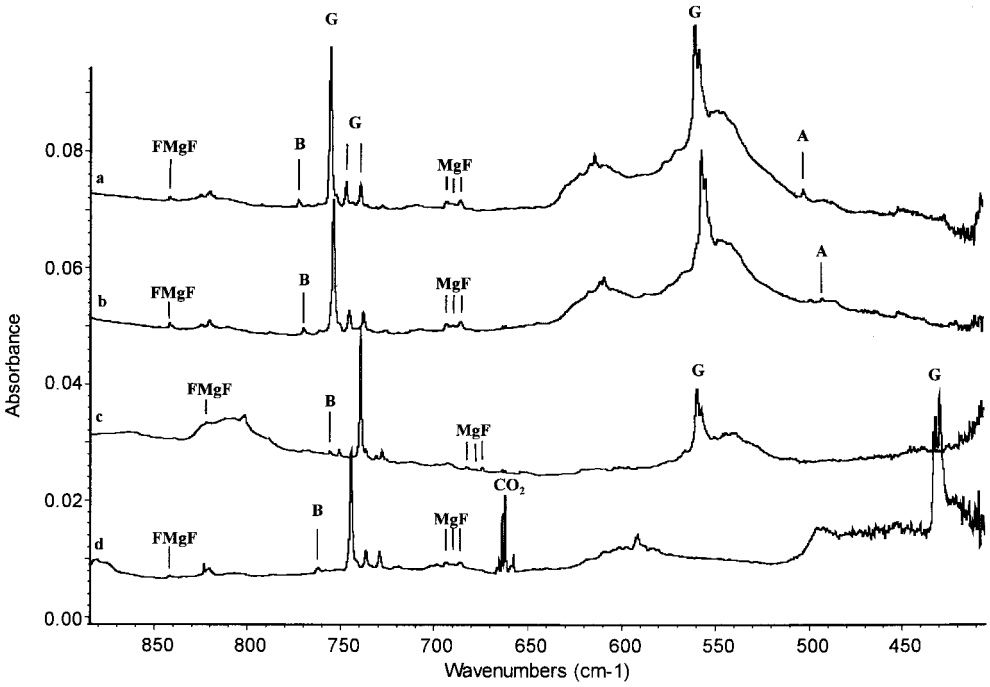

Figure 1. Infrared spectra in the 900−400 cm^{-1} region for products of reaction of methyl fluoride with laser-ablated magnesium atoms in solid argon: (a) $^nMg + CH_3F$, (b) $^nMg + {}^{13}CH_3F$, (c) $^{26}Mg + CH_3F$, and (d) $^nMg + CD_3F$.

A sharp, very weak band at 767.7 cm^{-1} was accompanied by two much weaker satellite bands at 758.9 and 750.9 cm^{-1}. These bands were unaffected by substitution with $^{13}CH_3F$ or CD_3X. Experiments with ^{26}Mg produced only the lowest of these bands. This band is due to OMgO as reported previously.[26] A sharp, very weak band was also observed at 943.0 cm^{-1}, which grew by 20% following each annealing cycle. The 943.0 cm^{-1} band was not affected by substitution with either $^{13}CH_3F$ or CD_3X, but was shifted to 931.9 cm^{-1} in experiments with ^{26}Mg. The 943.0 cm^{-1} absorption has been previously assigned to MgOMgO by Andrews and Yustein.[26]

A sharp band (**E**) at 1104.6 cm^{-1} was formed in experiments with all four methyl halides. The band was extremely weak in the CH_3F experiments, but increased with larger halogens, giving a relatively high yield for methyl iodide experiments. The band shifted to 1097.8 cm^{-1} with $^{13}CH_3F$. The band was not observed in the $^{26}Mg + CH_3F$ experiment, but was seen at 1103.6 cm^{-1} when ^{26}Mg was reacted with CH_3Cl.

A weak band was observed at 1421.6 cm^{-1} in all CH_3X experiments. The frequency of this band was not affected by $^{13}CH_3F$, but was shifted to 1419.8 cm^{-1} with ^{26}Mg and to 1037.7 cm^{-1} by CD_3F. These bands are due to MgH in solid argon.[27]

A broad band (**C**) was observed at 1561 cm^{-1}. This band was strongest in experiments with CH_3Cl, weaker with CH_3F,

(26) Andrews, L.; Yustein, J. T. *J. Phys. Chem.* **1993**, *97*, 12700.
(27) Tague, T. J., Jr.; Andrews, L. *J. Phys. Chem.* **1994**, *98*, 8611.

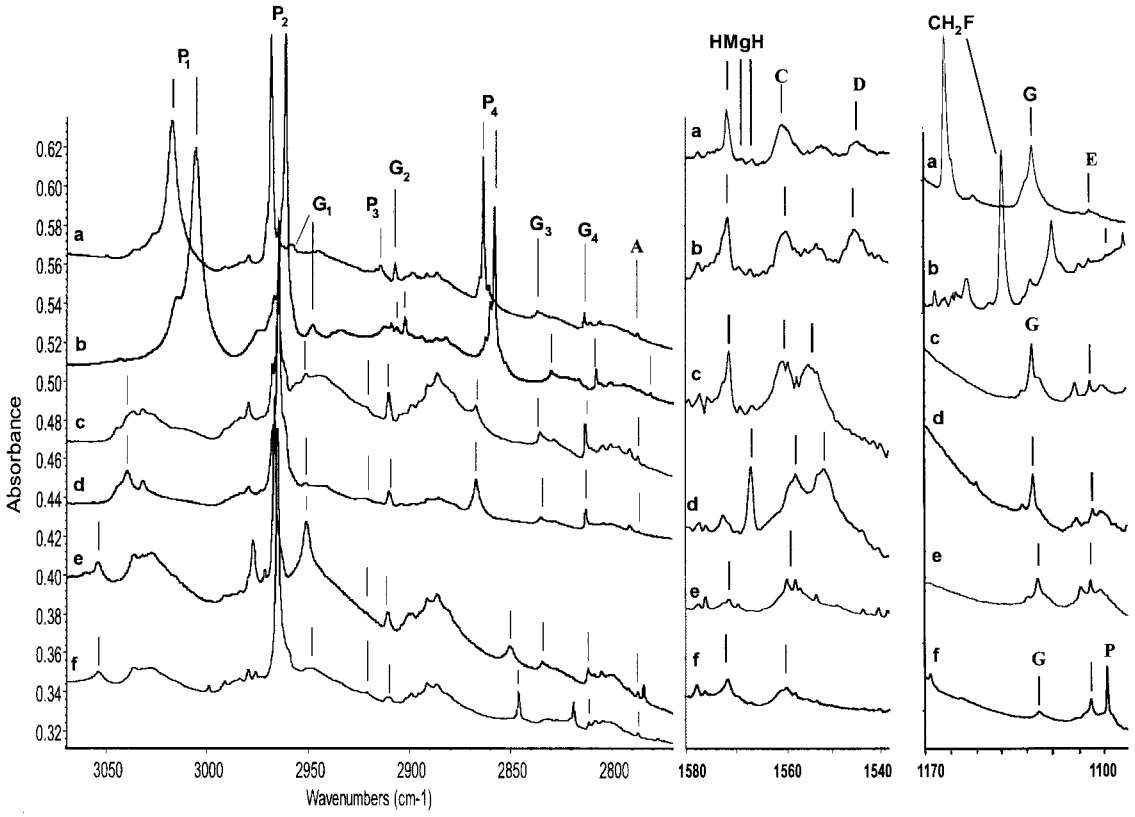

Figure 2. Infrared spectra in the 3070−2770, 1580−1540, and 1170−1100 cm^{-1} regions for reaction products of methyl halides with laser-ablated magnesium atoms in solid argon: (a) $^{n}Mg + CH_3F$, (b) $^{n}Mg + {}^{13}CH_3F$, (c) $^{n}Mg + CH_3Cl$, (d) $^{26}Mg + CH_3Cl$, (e) $^{n}Mg + CH_3Br$, and (f) $^{n}Mg + CH_3I$.

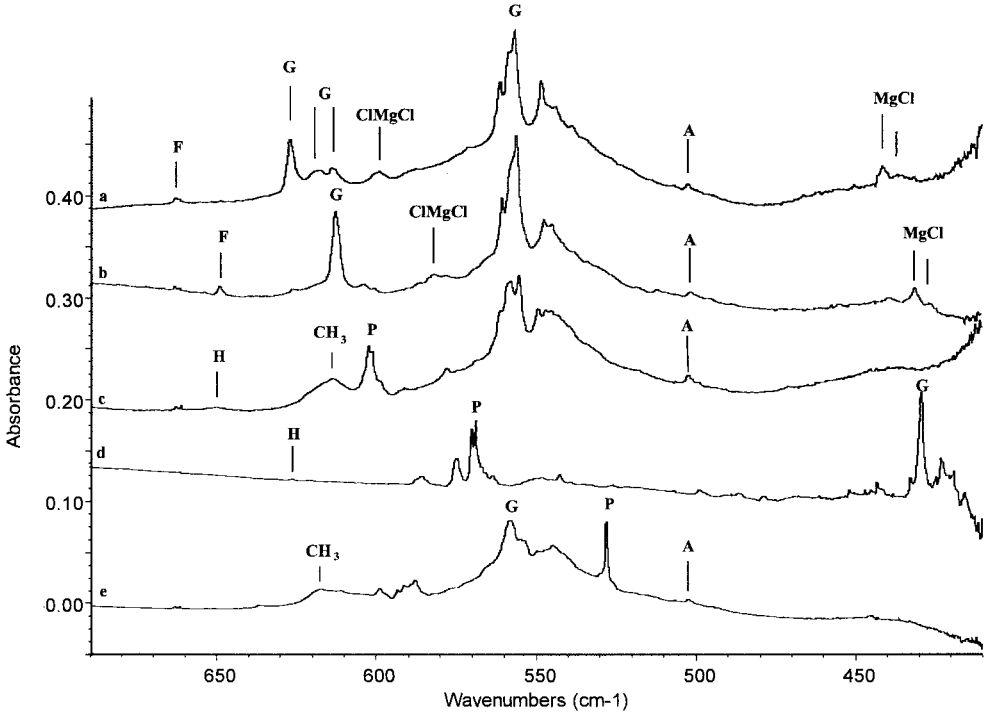

Figure 3. Infrared spectra in the 700−400 cm^{-1} region for reaction products of methyl halides with laser-ablated magnesium atoms in solid argon: (a) $^{n}Mg + CH_3Cl$, (b) $^{26}Mg + CH_3Cl$, (c) $^{n}Mg + CH_3Br$, (d) $^{n}Mg + CD_3Br$, and (e) $^{n}Mg + CH_3I$.

and quite weak for both CH_3Br and CH_3I. Isotopic shifts are reported in Table 3.

A sharp, weak triplet with an intensity ratio of 8:1:1 was observed at 1571.5, 1569.3, and 1567.2 cm^{-1}. These bands were unaffected by substitution with $^{13}CH_3F$, but were shifted to 1163.5, 1162.3, and 1161.0 cm^{-1} by CD_3F and by CD_3Br. Experiments with ^{26}Mg produced only the 1567.2 cm^{-1} band. These absorptions are due to HMgH as assigned by Tague and Andrews.[27]

In the C−H stretching region, a weak band (**A**) at 2787.1

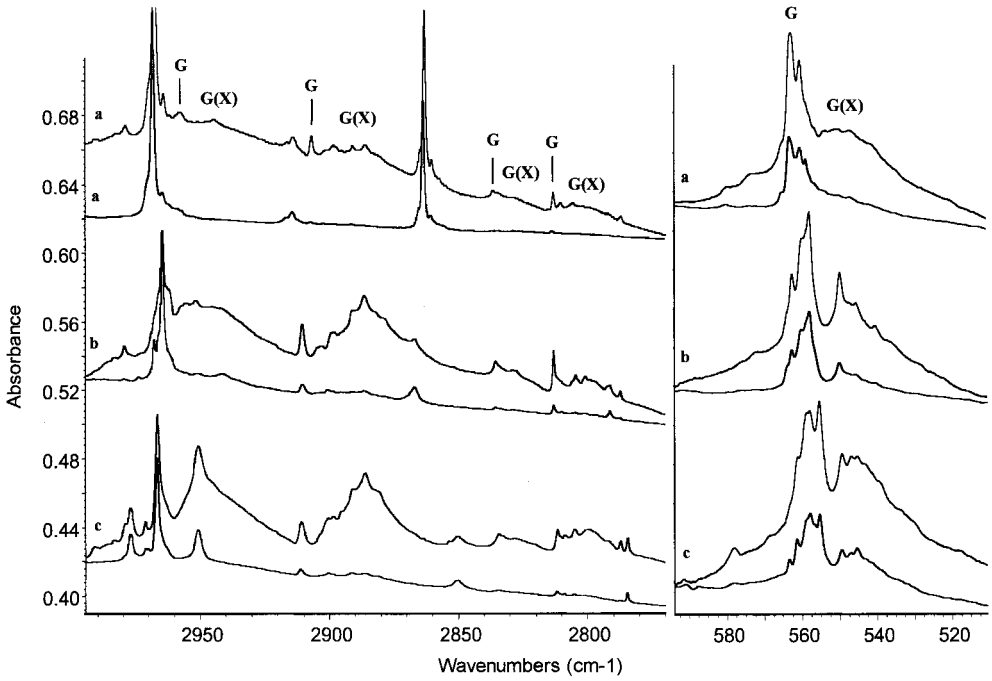

Figure 4. Infrared spectra in the 3000−2770 and 600−500 cm^{-1} regions for products of reactions of methyl halides with laser-ablated magnesium atoms at two different concentrations, showing bands due to isolated G and associated G(x) Grignard species. Each pair of spectra show products from reactions of 0.5% CH_3X (above) and 0.25% CH_3X (below) in argon: (a) $^nMg + CH_3F$, (b) $^nMg + CH_3Cl$, and (c) $^nMg + CH_3Br$.

Table 3. Infrared Bands (cm^{-1}) Observed in Experiments with All Methyl Halides

$^nMg + CH_3X$	$^{26}Mg + CH_3X$	$^nMg + {}^{13}CH_3X$	$^nMg + CD_3X$	assignment
502.2	494.9	492.1		**A**, $MgCH_2$[a]
767.7	750.9	767.7	767.7	OMgO
818.3	818.3	816.8	591.5	C_2H_6
820.3	820.3	818.9	592.6	C_2H_6
822.2	822.2	820.0	593.7	C_2H_6
943.0	931.9	943.0	943.0	MgOMgO
1104.6	1103.6	1097.8		**E**, CH_3MgCH_3
1305.4	1305.4	1297.5	993.7	CH_4
1374.6	1374.6			C_2H_6
1379.4	1379.4			C_2H_6
1421.9	1419.8	1421.6	1037.7	MgH
1464.3	1464.3			C_2H_6
1466.1	1466.1			C_2H_6
1467.9	1467.9			C_2H_6
1561	1559	1561	1136	**C**, $HMgCH_3$
1571.5, 1569.3, 1567.1	1567.1	1571.5	1163.5	HMgH
2787.1	2787.1	2781.3	2040.3	**A**, $MgCH_2$[a]
2891.4	2891.4	2887.2		C_2H_6
2979.7	2979.7			C_2H_6
3036.5	3036.5			CH_4

[a] Also observed in ref 25.

cm^{-1} was observed with all four methyl halides, and tracks with the band observed at 502.2 cm^{-1}. Isotopic shifts for this band are given in Table 3.

Mg + CH_3F. Experiments were conducted by using CH_3F, $^{13}CH_3F$, and CD_3F with ^nMg and CH_3F with ^{26}Mg. Spectra from these experiments are shown in Figures 1, 2, and 4, and infrared absorptions of different isotopic counterparts are listed in Table 4.

The most intense product band in the spectra resulting from the reaction of magnesium with methyl fluoride was a site-split band observed at 560.2 and 557.8 cm^{-1} (Figure 1). A strong, sharp triplet with an intensity ratio of 8:1:1 was observed at 755.8, 747.3, and 739.6 cm^{-1}. A moderately intense band was observed following deposition at 1127.2 cm^{-1}. Each of these bands (**G**) were shifted by isotopic substitution with ^{26}Mg, $^{13}CH_3F$, and CD_3F as described in Table 4.

A sharp band (**B**) was seen at 772.9 cm^{-1} following deposition. This band was shifted as a result of isotopic substitution with ^{26}Mg, ^{13}C, and D, as described in Table 4.

A collection of bands was formed on deposition at 693.5, 690.1, and 685.6 cm^{-1}. Low temperature (20 and 25 K) annealing decreased the first two sites, and high temperatures (30 and 35 K) decreased the third band. These bands were not shifted by substitution with $^{13}CH_3F$ or CD_3F but were shifted to 682.5, 678.3, and 674.1 cm^{-1} with ^{26}Mg.

The known MgF_2 band was observed at 842.2 cm^{-1}, and shifted to 822.5 cm^{-1} with ^{26}Mg, in agreement with earlier studies of thermally evaporated MgF_2 condensed in argon.[28−30]

Bands at 942.1, 922.2, and 912.8 cm^{-1} were observed following deposition and showed significant growth as a result of annealing. These bands were shifted by isotopic substitution as described in Table 4.

A sharp product band was seen at 1161.9 cm^{-1} following deposition. This band decreased markedly following both annealing and photolysis. The position of this band was unaffected by substitution with ^{26}Mg. Substitution of $^{13}CH_3F$ produced a 22.6 cm^{-1} red shift, and CD_3F yielded a 28.9 cm^{-1} *blue* shift to 1190.8 cm^{-1}, in agreement with earlier identification of the CH_2F radical by Raymond and Andrews.[31]

A broad absorption (**D**) was observed at 1547 cm^{-1}, which grew (15−20%) following each annealing cycle. Substitution with $^{13}CH_3F$ did not cause a measurable shift; isotopic counterparts with ^{26}Mg and D could not be determined, owing to low product yield.

Four halogen-dependent product bands (**G_1−G_4**) appeared in the C−H stretching region, which are shown in Figure 2 and listed in Table 7. CH_3F experiments produced two absorptions

(28) Snelson, A. *J. Phys. Chem.* **1966**, *70*, 3208.
(29) Mann, D. E.; Clader, G. V.; Seshardi, K. S.; White, D.; Linevsky, M. J. *J. Chem. Phys.* **1967**, *46*, 1138.
(30) Lesiecki, M. L.; Nibler, J. W. *J. Chem. Phys.* **1976**, *64*, 871.
(31) Raymond, J. I.; Andrews, L. *J. Phys. Chem.* **1971**, *75*, 3235.

Table 4. Infrared Bands Observed in Experiments with Methyl Fluoride Isotopic Molecules

$^{n}Mg + CH_3F$	$^{26}Mg + CH_3F$	$^{n}Mg + {}^{13}CH_3F$	$^{n}Mg + CD_3F$	assignment
546	539	542	421	**G**(**X**)
557.8	557.2	554.7	428.9	**G**, MeMgF Me rock (e)
560.2	559.6	557.0	431.3, 432.3	**G**, MeMgF Me rock, site (e)
685.8	674.1	685.8	685.8	MgF (site **A**)
690.0	678.3	690.0	690.0	MgF (site **B**)
693.5	682.5	693.5	693.5	MgF (site **C**)
739.6	739.6	737.9	729.2	**G**, $CH_3{}^{26}MgF$ antisym str (a_1)
747.3		745.7	736.5	**G**, $CH_3{}^{25}MgF$ antisym str (a_1)
755.8		754.1	744.5	**G**, $CH_3{}^{24}MgF$ antisym str (a_1)
772.9	756.1	770.2	762.9	**B**, $FMgCH_2$
822.5	822.5	822.5	822.5	$F^{26}MgF$
832.0		832.0	832.0	$F^{25}MgF$
842.2		842.2	842.2	$F^{24}MgF$
912.8	(913)	893.7	895.3	$(CH_3F)(Mg)$
922.8	922.0	902.4	903.8	$(CH_3F)(Mg)$
942.1	942.0	922.1	920.1	$(CH_3F)(Mg)$
1127.2	1127	1119.3	880.8	**G**, CH_3MgF sym Me def (a_1)
1161.9	1161.9	1139.3	1190.7	CH_2F (C−F str)
1547		1547		**D**, $HMgCH_2F$
2801	2805	2795	2046	**G**(**X**)
2813.3	2813.2	2808.1	2052.1	(**G**$_4$), CH_3MgF overtone (a_1)
2830	2829	2823		**G**$_3$(**X**)
2836.6	2836.5	2830.5		(**G**$_3$), CH_3MgF overtone (e)
2886	2891	2883	2195	**G**$_2$(**X**)
2907.2	2907.1	2902.8	2211.0	(**G**$_2$), CH_3MgF sym C−H str (a_1)
2947	2945	2935		**G**$_1$(**X**)
2958.5	2958 sh	2948.4	2232.6	(**G**$_1$), CH_3MgF antisym C−H str (e)

Table 5. Infrared Bands Observed in Experiments with ^{n}Mg and ^{26}Mg with CH_3Cl

$^{n}Mg + CH_3Cl$	$^{26}Mg + CH_3Cl$	assignment
441.2, 436.3	431.0, 426.2	MgCl
546	545	**G**(**X**)
556.6	556.3	**G**, CH_3MgCl Me rock (e)
561.3	560.8	**G**, CH_3MgCl Me rock (e)
599.4	582.1	ClMgCl
612.9	612.9	**G**, $CH_3-{}^{26}Mg-Cl$ antisym str (a_1)
618.0		**G**, $CH_3-{}^{25}Mg-Cl$ antisym str (a_1)
627.1		**G**, $CH_3-{}^{24}Mg-Cl$ antisym str (a_1)
663.0, 655.7, 649.3	649.3	**F**, $Cl-MgCH_2$
826.0	826.0	CH_2Cl (C−Cl str)
1127.5	1127.2	**G**, CH_3MgCl sym Me def (a_1)
1389.9	1389.9	CH_2Cl (CH_2 bend)
1555.4	1552.9	**D**, $HMgCH_2Cl$
2801	2801	**G**$_4$(**X**)
2812.8	2812.6	**G**$_4$, CH_3MgCl overtone (a_1)
2828	2827	**G**$_3$(**X**)
2835.3	2835.1	**G**$_3$, CH_3MgCl overtone (e)
2886	2886	**G**$_2$(**X**)
2910.4	2910.0	**G**$_2$, CH_3MgCl sym C−H str (a_1)
2946	2946	**G**$_1$(**X**)
2951.3	2951.3	**G**$_1$, CH_3MgCl antisym C−H str (e)

at 2958.5 and 2836.6 cm^{-1} and two sharper bands at 2907.3 and 2813.3 cm^{-1}.

Mg + CH$_3$Cl. Experiments were performed by using CH_3Cl with ^{n}Mg and ^{26}Mg. Spectra from these experiments are shown in Figures 2, 3, and 4, and bands are listed in Tables 5 and 7.

The strongest product band in the CH_3Cl experiments was an intense doublet at 561.3 and 556.7 cm^{-1}. Of slightly less intensity was a triplet with an 8:1:1 intensity ratio at 627.1, 619.8, and 612.9 cm^{-1}. A new band was observed at 1127.4 cm^{-1}, which resembled the 1127.2 cm^{-1} band in the CH_3F experiments in peak shape and intensity. Isotopic shifts for these bands (**G**) resulting from ^{26}Mg substitution are given in Table 5.

Table 6. Infrared Bands Observed in Experiments by Using ^{n}Mg with CH_3Br and CD_3Br

$^{n}Mg + CH_3Br$	$^{n}Mg + CD_3Br$	assignment
499	499	BrMgBr
546	422	**G**(**X**)
555.3	429.0	**G**, CH_3MgBr Me rock (e)
599 (sh)	575	$CH_3-Mg-Br$ antisym str (a_1) ?
650.9	626.4	**H**, $Br-MgCH_2$
696.2	655.7	CH_2Br (C−Br str)
1125.4	881.2	**G**, CH_3MgBr sym Me def (a_1)
1125.4	881.2	**G**, CH_3MgBr sym Me def (a_1)
1355	1015.8	CH_2Br (CH_2 bend)
2800	2049	**G**$_4$(**X**)
2811.5	2059.1	**G**$_4$, CH_3MgBr overtone (a_1)
2828		**G**$_3$(**X**)
2834.3		**G**$_3$, CH_3MgBr overtone (e)
2886	2105	**G**$_2$(**X**)
2910.6	2123.5	**G**$_2$, CH_3MgBr sym C−H str (a_1)
2944		**G**$_1$(**X**)
2950.9	2138.5	**G**$_1$, CH_3MgBr sym C−H str (a_1)

Table 7. Observed Frequencies (cm^{-1}) for Isolated Methyl Magnesium Halides in Solid Argon[a]

	CH_3MgF	CH_3MgCl	CH_3MgBr	CH_3MgI
Me rock (e)	560.2	556.6	555.3	558.2
antisym C−Mg−X str (a_1)	755.8	627.1	(599)	(588)
sym Me def (a_1)	1127.2	1127.5	1125.4	1125 br
Me def overtone (a_1)	2813.3	2812.8	2811.5	2811.1
Me def overtone (e)	2836.6	2835.3	2834.3	
sym C−H str (a_1)	2907.2	2910.4	2910.6	2910.3
antisym C−H str (e)	2958.5	2951.3	2950.9	2950 br

[a] Bands labeled G in the figures.

A moderately intense band was observed at 441.1 cm^{-1} with a sideband at 436.3 cm^{-1}. These bands shifted to 431.1 and 426.2 cm^{-1} with ^{26}Mg.

A broad absorption was observed at 599.3 cm^{-1}, which shifted to 582.3 cm^{-1} with ^{26}Mg. Bands in this region have been previously assigned to $MgCl_2$.[30]

A band (**F**) was observed following deposition at 663.0 cm^{-1},

along with two much weaker bands at 655.7 and 649.3 cm^{-1}. Although the band at 663.0 cm^{-1} is near the position of the ν_2 doublet of CO_2, this band showed no matrix splitting, and did not decrease on annealing as the band due to CO_2 does. When ^{26}Mg was used, only the lowest of these bands at 649.3 was observed.

A broad band (**D**) at 1555 cm^{-1} is seen in the Mg−H stretching region, which parallels the appearance and behavior of that seen at 1547 cm^{-1} discussed for CH_3F; however, the intensity of the band was much higher for CH_3Cl. ^{26}Mg shifted this band to 1553 cm^{-1}.

Bands were observed at 1389.9 and 826.0 cm^{-1}, which did not shift as a result of reaction with ^{26}Mg; these bands are due to the CH_2Cl radical, as assigned previously.[32]

Four new product bands (**G_1**−**G_4**, Figure 2) were observed in the C−H stretching region, which paralleled absorptions in CH_3F experiments.

Mg + CH_3Br. Experiments were conducted with CH_3Br and CD_3Br; spectra from these experiments are shown in Figures 2, 3 and 4, and bands are listed in Table 6.

The strongest product band in the CH_3Br experiments is a split band at 557.9 and 555.4 cm^{-1}. This band shifted to 428.1 cm^{-1} with CD_3Br. A 599 cm^{-1} shoulder on the CH_3Br band at 610 cm^{-1} apparently shifted to 575 cm^{-1} in experiments with CD_3Br. A broad band, observed at 1125.4 cm^{-1}, had a similar appearance to those seen with CH_3F and CH_3Cl in the same region. This band shifted to 881.2 cm^{-1} with CD_3Br.

A very weak band (**H**) was observed following deposition at 650.9 cm^{-1}, and was shifted to 626.4 cm^{-1} by substitution with CD_3Br.

Weak bands observed at 696.2 and 1355.0 cm^{-1}, which shifted to 655.7 and 1015.8 cm^{-1} with CD_3Br, are due to the CH_2Br radical, as assigned previously.[33] A broad band was observed at 1560 cm^{-1}. New product bands (**G_1**−**G_4**) in the C−H stretching region are shown in Figure 3 and listed in Table 7, as discussed for CH_3F and CH_3Cl.

Mg + CH_3I Spectra from experiments with ^{n}Mg and CH_3I are shown in Figures 2 and 3. Reactions with methyl iodide gave fewer product bands than the first three methyl halides. A broad band was observed at 558.2 cm^{-1} with sharper sidebands at 587.8 and 599.2 cm^{-1}. Very weak, broad bands were observed at 1125 and 1560 cm^{-1}. Weak absorptions (**G_1**) were observed in the C−H stretching region corresponding to bands in experiments with CH_3F, CH_3Cl, and CH_3Br, as listed in Table 7. Weak, sharp CH_2I radical bands were observed at 611.2 and 1331.2 cm^{-1}.[34] Methane and ethane absorptions were observed in slightly higher yields relative to other product bands.

Discussion

Spectral assignments are made on the basis of isotopic shifts and comparison with isotopic frequencies calculated by DFT.

CH_3MgX. Molecules with the Grignard structure (CH_3MgX) were observed in experiments with all four methyl halides. Bands labeled **G** assigned to the isolated CH_3MgX molecules are summarized in Table 7.

The absorptions at 755.8, 747.3, and 739.6 cm^{-1} in CH_3F experiments showed the natural abundance magnesium isotopic splitting pattern (8:1:1) characteristic of a vibration with significant Mg atom motion and agree well with the predicted frequency of the antisymmetric C−Mg−F stretch of CH_3MgF. An 8:1:1 natural magnesium isotope pattern was also clearly observed in the CH_3Cl experiments at 627.1, 619.8, and 612.9 cm^{-1}. These sets of bands are assigned to the antisymmetric C−Mg−X stretch of CH_3MgF and CH_3MgCl, respectively.

Intense, site-split bands were observed in the 555−560 cm^{-1} region in experiments with all four methyl halides. Bands in this region have previously been assigned[6] to the symmetric methyl deformation of CH_3MgX; however, DFT frequency calculations indicates that this assignment must be revised. The similarity of this band in all four methyl halide spectra indicate that the vibration responsible for this absorption must involve very little movement of the halogen atom. All four Grignard molecules are expected to have an intense, degenerate methyl rocking mode (with little halogen dependence) in this spectral region. Furthermore, matrix-splitting, as seen here, is common for degenerate vibrations, because matrix site asymmetry may cause a slight perturbation. Note also that the methyl rock of CH_3MgH has previously[25] been observed in solid argon at 547.9 cm^{-1}. Accordingly, the intense bands in this region are assigned to the degenerate methyl rocking motion of CH_3MgX.

The halogen-dependent, broad band near 1127 cm^{-1} for all methyl halides was shifted by substitution of ^{26}Mg (∼0.2 to 0.3 cm^{-1}), ^{13}C (∼8 cm^{-1}), and D (∼246 cm^{-1}). These isotopic shifts are consistent with the assignment of this band to the symmetric methyl deformation of the CH_3MgX molecules, which is calculated to be in this region. This band is predicted by DFT calculations to have a very low intensity, but is probably enhanced by interaction with the nearby (expected 1110 ± 10 cm^{-1}) overtone of the intense methyl rocking mode. However, it must be pointed out that infrared intensities are difficult to predict, and quantitative agreement between experiment and theory cannot be expected.

The antisymmetric methyl deformation, which has a low calculated IR intensity, was not observed in these experiments. The 1305 cm^{-1} band, which was assigned to this vibration by Ault,[6] differs (by ∼130 cm^{-1}) with the DFT calculations, which are more accurate for other frequencies. The 1305 cm^{-1} band reported previously is probably due to methane.

An analysis of the C−H stretching region (Figure 2) requires an understanding of the infrared spectra of the parent methyl halide molecules, which have been described for CH_3F by Young and Moore.[35] Bands labeled **P_1** and **P_2** are due to the antisymmetric (e) and symmetric (a_1) C−H stretching modes, respectively, of the CH_3X molecules. Note that in all cases, the a_1 mode is much sharper and stronger than the e mode. Also, the ^{13}C-shift (shown for CH_3F) of the e mode (10.9 cm^{-1}) is approximately double that of the a_1 mode (6.0 cm^{-1}), as predicted by calculations. Bands labeled **P_3** and **P_4** are not due to C−H stretching motions, but are unusually strong overtone bands involving the methyl deformation modes. The overtones have components of appropriate symmetry to interact with the C−H stretching modes of like symmetry causing Fermi resonance enhancement of the overtone absorption intensities. Insofar as these interacting modes primarily involve the methyl group, we expect to see similar behavior (with reduced halogen dependence) for the Grignard molecules.

The product bands **G_1**−**G_4** are slightly halogen dependent, and also show isotopic shifts resulting from ^{13}C, D, and ^{26}Mg substitution. The ^{13}C isotopic shifts (9.9 and 4.5 cm^{-1}) for **G_1** and **G_2** in the CH_3F experiment clearly identify e and a_1 modes, respectively. These bands are assigned to the antisymmetric and symmetric C−H stretching modes of the Grignard molecules. Isotopic shifts for bands **G_3** and **G_4** are complicated by mode mixing, but are nevertheless comparable to those of **P_3**

(32) Andrews, L.; Smith, D. W. *J. Chem. Phys.* **1970**, *53*, 2956.
(33) Smith, D. W.; Andrews, L. *J. Chem. Phys.* **1971**, *55*, 5295.
(34) Smith, D. W.; Andrews, L. *J. Chem. Phys.* **1973**, *58*, 5222.
(35) Young, L.; Moore, C. B. *J. Phys. Chem.* **1982**, *76*, 5869.

and **P_4**. These bands are therefore assigned as the e and a_1 components of the antisymmetric methyl deformation overtone, supported by comparison with the parent methyl halide molecule.

Four broad (full-width at half-maximum = 20−50 cm^{-1}) absorptions (**G(X),** Figure 4) were observed in experiments with all methyl halides. These bands at 540, 2800, 2830, 2880, and 2940 cm^{-1} are slightly red-shifted relative to sharp bands assigned here to the methyl rock, the C−H stretches, and the methyl deformation overtone bands of the isolated Grignard molecules. These broad bands agree with IR bands reported by Ault[6] and by Solov'ev et al.[7] from thermal Mg atom experiments. Our laser-ablation experiments were repeated with more dilute (0.25%) methyl halide samples, resulting in a significant attenuation of these broad absorptions relative to the neighboring sharp bands. We believe that the sharp bands observed here are due to the isolated Grignard molecules, while the broad bands are actually due to Grignard molecules aggregated with additional methyl halide molecules or magnesium clusters.

(CH_3F)(Mg). Several peaks in the 910−940 cm^{-1} region were observed in experiments with CH_3F. These bands (942.1, 922.2, and 912.8 cm^{-1}) show isotopic shifts which are similar to those of the C−F stretch of CH_3F and are about 100 cm^{-1} to the red of the CH_3F vibration. This band is assigned as the perturbed C−F stretch in the van der Waals complex (CH_3F)-(Mg), which was predicted by BP86 calculations to have an intense C−F vibration at 978.0 cm^{-1} with isotopic shifts near those observed here.

The observed growth of these bands on annealing is also consistent with assignment to an unreacted reagent complex, (CH_3F)(Mg), which likely forms as Mg atoms diffuse in the argon matrix. The formation of this complex, and not the CH_3-MgF Grignard species, on annealing is noteworthy and indicates that excited Mg atoms are required for the reaction leading to CH_3MgF. Analogous bands were not observed in experiments with CH_3Cl, CH_3Br, or CH_3I.

$HMgCH_3$. A broad, halogen-independent band (**C**) was observed at 1561 cm^{-1} in all experiments. This band is in the region expected for a Mg−H stretch, and shows isotopic shifts ($\Delta C = <1$ cm^{-1}, $\Delta Mg = 2$ cm^{-1}) which are consistent with assignment to $HMgCH_3$. The Mg−H stretch of $HMgCH_3$ has been previously reported at 1524 cm^{-1} in solid methane[36] and at 1561 cm^{-1} in solid argon.[25]

CH_3MgCH_3. A weak halogen-independent band observed at 1104.6 cm^{-1} is probably due to the out-of-phase symmetric methyl deformation of CH_3MgCH_3. The position of this band is near the methyl deformation absorptions of CH_3MgH (1127.7 cm^{-1}) and CH_3MgX (∼1125−1127 cm^{-1}), and the observed 6.8 cm^{-1} ^{13}C shift is consistent with this assignment; the 1104.6 cm^{-1} band does not track with other bands observed here, and it was not observed in methane experiments.[25] The 1.0 cm^{-1} ^{26}Mg shift is larger than expected on the basis of calculations; however, the band due to CH_3MgH, previously observed at 1127.7 cm^{-1}, also shows a ^{26}Mg shift which is substantially larger than that predicted by DFT calculations.[25] The CH_3-$MgCH_3$ species is expected to have two intense IR bands near 600 cm^{-1}. Although broad bands in this region exhibit isotopic shifts which are appropriate for this molecule, this is a rich spectral region, and interference from bands due to CH_3, CH_3-MgCl, $MgCl_2$, and CH_3Br has made identification of halogen-independent bands difficult. Alternative assignments for this band, including $MgCH_3$, cannot be excluded. Weak, neighboring halogen-dependent bands (1110.3 cm^{-1}, Cl; 1108.5 cm^{-1}, Br; 1096.1 cm^{-1}, I) may be due to CH_3MgCH_2X species.

$HMgCH_2X$. Broad, halogen-dependent bands (**D**) were observed in the Mg−H stretching region in experiments with methyl fluoride (1547 cm^{-1}) and methyl chloride (1555 cm^{-1}). As with $HMgCH_3$, no measurable ^{13}C shift and a 2 cm^{-1} ^{26}Mg shift were observed. No bands due to $HMgCH_2Br$ or $HMgCH_2I$ were observed.

CH_2X. Experiments with all four methyl halides produced the monohalomethyl radicals, CH_2F, CH_2Cl, CH_2Br, and CH_2I, which were identified from previous work.[31−34] Product yields were highest for CH_2F and lowest for CH_2I. A weak, broad methyl radical band[37] was observed with CH_3Br and CH_3I.

MgX. Both MgF and MgCl were formed as products in these reactions. In experiments with CH_3F, the collection of bands at 693.5, 690.1, and 685.8 cm^{-1} were shifted to 682.3, 678.3, and 674.1 cm^{-1} with ^{26}Mg, giving isotopic frequency ratios of 1.01642, 1.01736, and 1.01736, respectively. These are all in excellent agreement with the harmonic diatomic ratio of 1.01744, and with the 675.1 cm^{-1} frequency predicted for ^{24}MgF by B3LYP calculations. In CH_3Cl experiments, the band at 441.1 cm^{-1} with a 436.3 cm^{-1} sideband was shifted to 431.1 and 426.2 cm^{-1} by ^{26}Mg, giving two $^{24}Mg/^{26}Mg$ isotopic frequency ratios of 1.02367 and 1.02370 and two $^{35}Cl/^{37}Cl$ ratios of 1.01100 and 1.01150. The expected harmonic diatomic ratios are 1.02343 (24,35/26,35) and 1.01117 (24,35/24,37). B3LYP calculations have predicted the $^{24}Mg^{35}Cl$ fundamental at 437.4 cm^{-1}. These bands are slightly red-shifted relative to the gas-phase fundamentals (702 and 458 cm^{-1} for MgF and MgCl, respectively),[38] as is expected for diatomic molecules in a matrix environment. Although an ESR study of MgF in solid argon has been reported,[39] we do not know of any matrix infrared assignments for these molecules.

Other Bands. The bands at 502.2 and 2787.1 cm^{-1} will be assigned to $MgCH_2$ and the 772.9, 663.0, and 650.9 cm^{-1} bands to $XMgCH_2$ species in a later experimental and theoretical study.

Reaction Mechanisms. Most products in the laser-ablation experiments were observed following deposition, rather than on subsequent annealing or photolysis. These Mg atom reactions occur during deposition in the condensing layer on the matrix surface. This suggests that excited Mg atoms (^3P) are involved here,[40,41] in contrast to the early work of Skell and Girard with thermal ground-state Mg atoms (^1S), where reaction occurred on warming the neat Mg/alkyl halide samples.[42] Products observed following reactions of laser-ablated magnesium atoms with methyl halides are believed to form by three major mechanisms.

The first reaction pathway is initiated by insertion of an excited magnesium atom into the C−X bond of the parent methyl halide, forming an excited [CH_3MgX]* molecule, as in reaction 1. A UV−vis study by Imizu and Klabunde has shown that ground-state magnesium atoms, Mg(^1S), are not reactive toward methyl halide molecules.[5] Laser ablation, however, produces a significant population of excited, triplet state magnesium atoms.[40] The lifetime of Mg (^3P) state atoms (2 ms)[41] is much longer than the time-of-flight for hyperthermal

(36) McCaffrey, J. G.; Parnis, J. M.; Ozin, G. A.; Breckenridge, W. H. *J. Phys. Chem.* **1985**, *89*, 4945.

(37) Milligan, D. E.; Jacox, M. E. *J. Chem Phys.* **1967**, *47*, 5146.

(38) Huber, K. P.; Herzberg, G. *Constants of Diatomic Molecules*.; Van Nostrand: New York. 1979.

(39) Knight, L. B., Jr.; Easley, W. C.; Weltner, W., Jr.; Wilson, M. *J. Chem. Phys.* **1971**, *54*, 322.

(40) Andrews, L.; Chertihin, G. V.; Thompson, C. A.; Dillon, J.; Byrne, S.; Bauschlicher, C. W., Jr. *J. Phys. Chem.* **1996**, *100*, 10088.

(41) Husain, D. *J. Chem. Soc., Faraday Trans. 2* **1989**, *85*, 85.

(42) Skell, P. S.; Girard, J. E. *J. Am. Chem. Soc.* **1972**, *94*, 5518.

Mg atoms, and so, triplet magnesium atoms may reasonably be involved in this reaction. The insertion of Mg (^{3}P) into the C−X bond is expected to be more exothermic than that of Mg (^{1}S) by the 62.5 kcal/mol excitation energy.[41]

$$Mg(^3P) + CH_3X \rightarrow [CH_3MgX]^* \quad (1)$$

Once formed, the activated $[CH_3MgX]^*$ species may relax to give the Grignard molecule (reaction 1a) or may further decompose to give CH_3, CH_3Mg, $MgCH_2$, MgX, HX, and/or X (reactions 1b−1e)

$$[CH_3MgX]^* \rightarrow CH_3MgX \quad (1a)$$

$$[CH_3MgX]^* \rightarrow CH_3 + MgX \quad (1b)$$

$$[CH_3MgX]^* \rightarrow MgCH_2 + HX \quad (1c)$$

$$[CH_3MgX]^* \rightarrow CH_3Mg + X \quad (1d)$$

$$[CH_3MgX]^* \rightarrow CH_2MgX + H \quad (1e)$$

As one might anticipate, the formation and trapping of Grignard species in these experiments showed a clear trend. The reaction was most efficient for CH_3F, less efficient for CH_3Cl and CH_3Br, and least efficient for CH_3I, which produced broader bands and a very low yield of CH_3MgI. This supports the formation mechanism proposed above in that the trend parallels Mg−X bond strength, and indicates that the tendency for the $[CH_3MgX]^*$ complex to decompose increases with decreasing Mg−X bond strength. It is illustrative to compare the relative intensities of the 1127 cm^{-1} (**G**, CH_3MgX) and 1104 cm^{-1} (**E**, CH_3MgCH_3) bands (Figure 2) for CH_3F and CH_3I. As expected, CH_3MgF is the major product in the CH_3F experiments, and the halogen-independent product is favored with CH_3I.

The second reaction pathway is initiated by insertion of an excited magnesium atom into a the C−H bond of CH_3X, yielding an activated $[HMgCH_2X]^*$ species, as in reaction 2.

$$CH_3X + Mg(^3P) \rightarrow [HMgCH_2X]^* \quad (2)$$

Relaxation of this excited molecule leads to formation of $HMgCH_2X$ (reaction 2a), and decomposition may form MgH and CH_2X as in reaction 2b or possibly the $MgCH_2$ intermediate as in reaction 2c.

$$[HMgCH_2X]^* \rightarrow HMgCH_2X \quad (2a)$$

$$[HMgCH_2X]^* \rightarrow MgH + CH_2X \quad (2b)$$

$$[HMgCH_2X]^* \rightarrow MgCH_2 + HX \quad (2c)$$

The $HMgCH_2X$ species were observed only for fluorine and chlorine, which is likely a result of the comparatively high C−X bond strength for fluorine and chlorine relative to bromine and iodine, as discussed above for CH_3MgX. Bromine- and iodine-containing molecules may be more likely to decompose to other products. Monohalomethyl radicals, CH_2X, were observed for all halogens.

The third likely reaction pathway is photolytic cleavage of the C−X bond of CH_3X (reaction 3), and subsequent addition of radicals in the matrix (reactions 3a−3f).

$$CH_3X\ (h\nu) \rightarrow CH_3 + X \quad (3)$$

The photolysis of alkyl halides is well-known, and the UV radiation given off by the laser plume in experiments of this type is certainly capable of inducing methyl halide photodissociation. This reaction path is likely to be most important for CH_3Br and CH_3I, which are most easily photolyzed.

$$CH_3 + CH_3 \rightarrow C_2H_6 \quad (3a)$$

$$CH_3 + Mg \rightarrow CH_3Mg \quad (3b)$$

$$HMg + CH_3 \rightarrow HMgCH_3 \quad (3c)$$

$$HMg + CH_2X \rightarrow HMgCH_2X \quad (3d)$$

$$CH_3 + MgCH_3 \rightarrow CH_3MgCH_3 \quad (3e)$$

$$CH_3F + Mg \rightarrow (CH_3F)(Mg) \quad (3f)$$

Insofar as most bands showed little growth on annealing, these secondary (radical recombination) reactions are a minor route, relative to decomposition of larger species. However, annealing growth was seen for the band ascribed to $HMgCH_2X$, indicating that radical recombination is one path by which that molecule is formed. Also, some recombination of radicals is to be expected in the condensing matrix phase during deposition as is evidenced by the formation of ethane in all experiments. As expected, the yield of ethane, relative to other products, was highest for methyl iodide and lowest for methyl fluoride. Finally, the van der Waals complex is made by association of cold reagents in the case of the less reactive methyl fluoride.

Conclusions

Excited magnesium atoms were generated by laser ablation and reacted with methyl halides diluted in argon. Reaction products were trapped in a cryogenic argon matrix and analyzed by infrared spectroscopy. Reaction products, which included the isolated Grignard molecules CH_3MgX and subsequent MgX, MgX_2, MgH, MgH_2, CH_4, C_2H_6, CH_2X, $HMgCH_3$, $XMgCH_2$, CH_3MgCH_3, and $HMgCH_2X$ species, were identified by isotopic (^{13}C, D, and ^{26}Mg) substitution and by correlation with B3LYP and BP86 frequency calculations. This investigation reports the first experimental evidence for the fluoride Grignard molecule CH_3MgF. Infrared absorptions were also observed for Grignard species associated with other molecules.

Although calculations have indicated that dimagnesium Grignard species (i.e. CH_3MgMgX and CH_3MgXMg) may be thermodynamically stable, products of this type were not observed.

Acknowledgment. We gratefully acknowledge support for this research from N.S.F. Grant No. CHE 97-00116.

JA980806N